Sensors and Materials, Vol. 34, No. 6 (2022) 2065–2074
MYU Tokyo

LETTER

S & M 2956

Fabrication and Humidity Sensing of Reduced Graphene Oxide/Polyaniline Composite Film on Flexible Paper Substrate

Yonggang Du,[1*†] Xiuhua Li,[2†] Xinhui Zhao,[3†] Ning Wang,[1†] and Dailin Li[1†]

[1]College of Science, China University of Petroleum (East China),
No. 66 Changjiang West Road, Qingdao, Shandong 266580, China
[2]State Key Laboratory of Precision Spectroscopy, East China Normal University, Shanghai 200062, China
[3]State Key Laboratory of Advanced Optical Communication Systems and Networks,
School of Physics and Astronomy, Shanghai Jiao Tong University, Shanghai 200240, China

(Received January 12, 2022; accepted March 30, 2022)

Keywords: reduced graphene oxide, polyaniline, paper substrate, filtration, humidity sensing

We present a flexible humidity sensor comprising a reduced graphene oxide/polyaniline (RGO/PANI) composite film on a polypropylene filter paper substrate. Graphene oxide was reduced with sodium borohydride ($NaBH_4$), then PANI was prepared by the oxidative polymerization of aniline to produce the RGO/PANI composite. The suspension of the as-prepared RGO/PANI composite was simply filtered on the paper substrate for sensor fabrication. The structure and morphology of the obtained composite were investigated by SEM, Fourier transform IR spectroscopy, and Raman spectroscopy. The experimental results revealed that the RGO/PANI composite film on the paper substrate can be used for humidity sensing with low hysteresis, good repeatability, and a large response in a broad humidity range. Moreover, our sensor has the potential to be applied in wearable devices because of the flexible substrate.

1. Introduction

In recent years, humidity sensing has played an important role in various applications, such as weather forecasting, industrial production, medical instruments, and agricultural planting.(1) The performance of a humidity sensor depends critically on the characteristics of its sensing materials. So far, a series of materials have been employed in humidity sensing, including metal oxides, polymer electrolytes, and carbon nanotubes.(2)

Graphene, a very attractive 2D carbon nanomaterial with excellent mechanical flexibility, high surface area, and low manufacturing cost, has been widely used in fields such as biology, medicine, and gas sensing.(3) Graphene oxide (GO), an important derivative of graphene, has multiple chemical groups containing oxygen that can enhance the hydrophilicity and introduce abundant adsorption sites of water molecules, endowing GO with the ability to detect humidity. Nevertheless, these groups disrupt the sp^2 structure of graphene and make it electrically insulating. Thus, the electrical characteristics of GO are difficult to measure, which is a hindrance for humidity sensing. Reduced graphene oxide (RGO) is a potential candidate for

*Corresponding author: e-mail: duyg@upc.edu.cn
†These authors contributed equally to this paper and should be considered co-first authors.
https://doi.org/10.18494/SAM3793

ISSN 0914-4935
https://myukk.org/

various types of humidity sensors since chemical reduction processes can restore its conductivity while still keeping the chemically active defect sites.[4] However, RGO tends to aggregate and stack owing to π–π interactions and van der Waals forces, severely decreasing the effective specific surface area. As a result, a pure RGO humidity sensor usually exhibits a low response even at high humidity.[5]

Many studies have shown that sensors based on two materials mixed together may show improved humidity-sensing properties due to the synergistic effect between the two components.[6] Wang *et al*. fabricated reduced graphene oxide–polyethylene oxide (RGO-PEO) nanocomposites for humidity detection. The humidity sensitivity of the RGO-PEO composite was found to be twice that of the pure PEO.[7] Li *et al*. synthesized a QC-P4VP/PANI humidity sensor, which exhibited lower hysteresis than that of a sensor based on only QC-P4VP.[8] These studies inspired us to design a composite to improve the humidity-sensing performance of RGO.

Electrically conducting polymers such as polyaniline (PANI) have been used to fabricate humidity sensors because their physical and chemical properties can be easily modulated by simple fabrication. However, pure PANI has limited applicability as a humidity sensor owing to its intrinsic instability under high humidity conditions and its large hysteresis.[9] Therefore, we decided to fabricate a humidity sensor based on an RGO/PANI composite to combine the advantages of both RGO and PANI.

The RGO/PANI composite has also been widely applied in research on supercapacitors. However, the effects of humidity on the performance of supercapacitors based on the RGO/PANI composite have not yet been fully considered. In fact, humidity has a significant effect on the utilization of supercapacitors. For example, it has been reported that the capacity of a supercapacitor using RuO_2 varies greatly with the humidity level, and the cycle lifetime of the supercapacitor is poor in a high-humidity environment.[10] Research on the humidity-sensing properties of the RGO/PANI composite could also provide guidelines for the application of supercapacitors based on this composite.

At present, humidity sensor devices are usually manufactured on ceramic and crystalline silicon substrates with interdigitated electrodes. However, the interdigitated electrodes are usually fabricated via high-cost and sophisticated nanolithography techniques, which hamper the development and application of humidity sensors. At the same time, solid-state substrates suffer from poor mechanical flexibility, which restricts their application in flexible electronic devices such as wearable devices. Paper is considered a potential substrate for low-cost flexible electronics because of its multiple advantages including flexibility, portability, and low cost.[11] In this study, our humidity sensor is fabricated on a paper substrate, giving it the potential to be further applied in wearable devices.

Although many humidity sensors have already shown a high response at a high relative humidity (RH) level, the response at a low RH level (<30%) has not been satisfactory.[12] Developing a cost-effective humidity-sensing material that exhibits a high response in the full range of RH is still a challenge.

In this work, we aim to fabricate a flexible humidity sensor comprising an RGO/PANI composite film on a polypropylene filter paper substrate. The humidity-sensing properties of the as-prepared sensor are investigated and the experimental results indicate that the combination of

RGO and PANI leads to improved humidity-sensing performance, including a high response, low hysteresis, and good repeatability. More importantly, the RGO/PANI composite film is sensitive in almost the whole RH range (0–98%).

2. Experiment

2.1 Materials and chemicals

Ammonium persulfate (APS, ≥98%), hydrochloric acid (HCl, 37%), aniline (C_6H_7N, ≥99.9%), and sodium borohydride ($NaBH_4$, 98%) were purchased from Aladdin. GO (thickness: 0.8–1.2 nm, diameter: 0.5–5 μm) was obtained from Nanjing XFNANO Materials Tech Co., Ltd. All reagents were used as received without any previous treatment. Silver conductive paint (05001-AB, sheet resistivity: <100 mΩ/square, volume resistivity: 3×10^{-5} Ω·cm) was purchased from SPI Co., USA.

2.2 Fabrication of sensor

RGO was prepared by chemically reducing GO with $NaBH_4$. Briefly, 55 mg of GO was dissolved in 200 ml of deionized water and then treated with ultrasonic waves for 0.5 h to obtain a homogeneous solution. Subsequently, 20 ml of deionized water containing 500 mg of $NaBH_4$ was added to the as-prepared GO solution, and the whole solution was magnetically stirred at 80 °C for 1.5 h to obtain an RGO suspension. Finally, the RGO was collected by filtering and dried under vacuum at 60 °C for 5 h.

PANI was prepared by chemical oxidative polymerization with APS used as the oxidant. Typically, the as-prepared RGO (5 mg), aniline (0.044, 0.093, or 0.191 mL), and HCl (1 M) were mixed and then APS (0.1099, 0.2322, or 0.477 g) was added. The weight feed ratio of aniline to RGO was 90:10, 95:5, or 97.5:2.5 and the resulting hybrids were named PRG10, PRG5, and PRG2.5, respectively. Next, the as-prepared solution was magnetically stirred for 1.5 h in an ice-water bath (0–5 °C). Finally, the dark green precipitate was separated from the solution by filtration and the RGO/PANI nanocomposite was obtained after drying in vacuum at 60 °C for 5 h.

To prepare the humidity sensor, 5 mg of the as-prepared RGO/PANI composite with each of the different proportions was added to 20 mL of ethanol. Afterwards, the resulting solutions were ultrasonically stirred for 1 h to completely dissolve the composite. Subsequently, the as-prepared solutions were filtered through a polypropylene filter paper with a pore size of 0.22 μm, forming an RGO/PANI composite film on the paper substrate. Figures 1(a) and 1(c) show a schematic diagram and a photo of the RGO/PANI humidity sensor, respectively. The electrodes were prepared by brushing conductive Ag paste onto the film and connecting copper wires. The distance between the Ag electrodes was about 2 mm to ensure ease of preparation and moderate resistance value of the RGO/PANI humidity sensor. The dimensions of the paper and the Ag electrode were about 10×10 mm^2 and 2×8 mm^2, respectively.

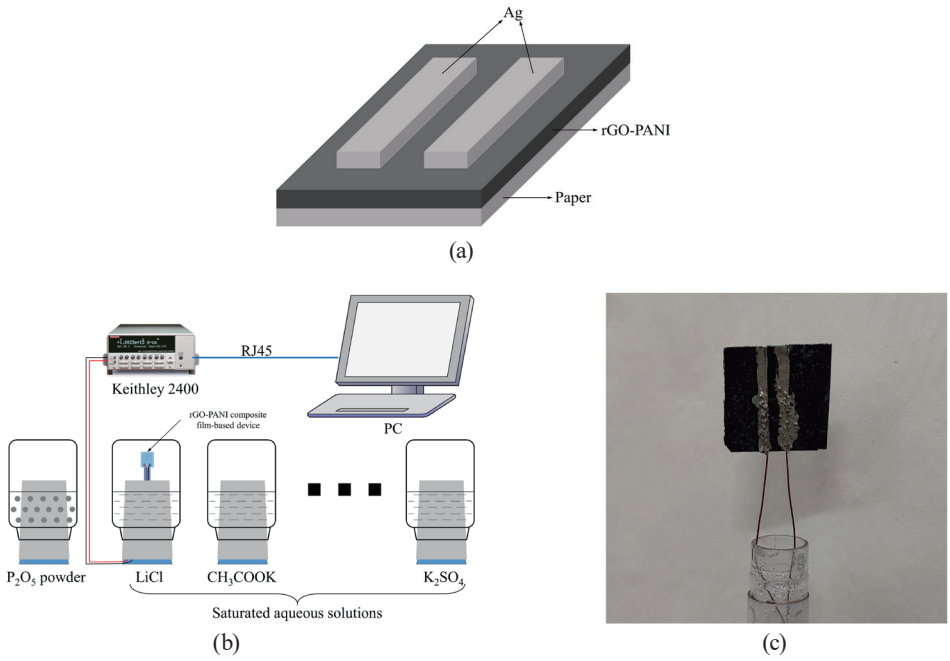

Fig. 1. (Color online) (a) Schematic illustration of the paper substrate sensor. (b) Schematic illustration of humidity-sensing measurement setup. (c) Photo of the fabricated sensor.

2.3 Experimental setup

A schematic illustration of the humidity-sensing measurement setup is shown in Fig. 1(b). The electrical characteristics of the as-prepared RGO/PANI humidity sensor were measured using a Keithley 2400 sourcemeter. The humidity-sensing performances were studied by placing the RGO/PANI humidity sensor in a series of RH environments at room temperature (~25 ± 1 °C). A series of saturated salt solutions of LiCl, CH_3COOK, $MgCl_2$, K_2CO_3, $Mg(NO_3)_2$, KI, NaCl, KCl, and K_2SO_4 were used to achieve and maintain RH levels of 11, 22, 33, 43, 54, 69, 75, 84, and 98%, respectively. P_2O_5 powder was used as a desiccant to generate 0% RH.

The response R is an important parameter for evaluating the performance of the humidity sensor, which is defined as $R = (I_{RH} - I_0)/I_0 \times 100\%$, where I_{RH} and I_0 are the currents of the humidity sensor at a particular RH and 0% RH, respectively. The times needed to attain 90% of the total current change during the humidification and desiccation processes are defined as the response and recovery times, respectively.[13]

3. Experimental Results and Discussion

3.1 Morphology and characterization

The morphologies of the RGO/PANI film are shown in Fig. 2. Figure 2(a) shows that the PANI nanofibers have a porous structure. Figure 2(b) shows that the structure of the RGO/PANI

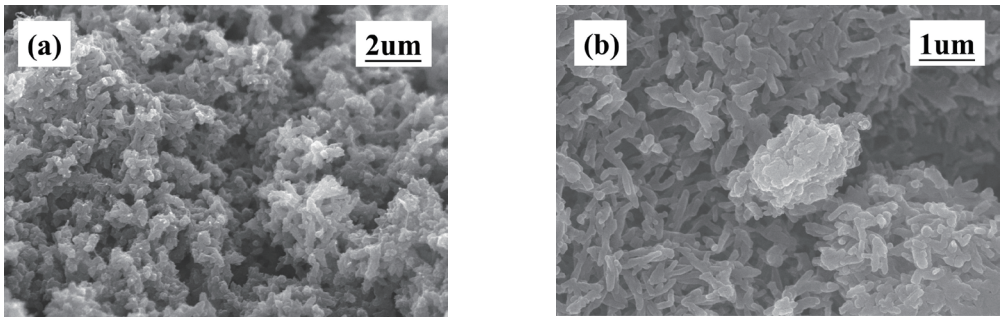

Fig. 2. SEM images of (a) pure PANI film and (b) RGO/PANI film.

film is meshed and that the fiber dimension belongs to the nanometer range. The meshed nanofibers of PANI are closely combined with the RGO nanosheets, and the RGO nanosheets are homogeneously surrounded by PANI nanofibers.[14]

The structures of the as-prepared pure PANI and the RGO/PANI composite were examined by Fourier transform IR (FTIR) spectroscopy. As can be seen in Fig. 3(a), the spectrum of the RGO/PANI composite clearly shows absorption at 1562 and 1481 cm^{-1} due to C=C stretching of the quinoid and benzenoid rings, respectively. The characteristic peaks observed at 1295 and 1133 cm^{-1} correspond to C–N stretching of secondary aromatic amines and C=N stretching vibration, respectively. The band characteristic of the benzene ring out-of-plane bending vibration of the C–H group is located at 802 cm^{-1}.[15] The characteristic peaks of PANI are similar to those of the RGO/PANI composite, which suggests that both have similar structures because the content of PANI is higher than that of RGO. In addition, compared with PANI, almost all the absorption peaks of PANI/RGO have a small shift in the IR direction. This may be due to the formation of hydrogen bonds between PANI and RGO, which demonstrates the successful incorporation of RGO in the RGO/PANI composite.[16]

To further determine the structures of PANI and the RGO/PANI composite, Raman spectra were measured, as displayed in Fig. 3(b). For pure PANI, the peaks centered at 1583 and 1460 cm^{-1} are respectively attributed to C–C stretching of the benzoid and C=N stretching of the emeraldine base. The relatively weak peak at 1331 cm^{-1} is ascribed to C–N stretching. The bands at 1211 and 1161 cm^{-1} are related to in-plane ring deformation and C–H bending of the quinoid ring, respectively. The peaks observed at 813, 517, and 416 cm^{-1} are assigned to bipolaronic quinoid ring deformation, out-of-plane C–H wag, and C–N–C torsion, respectively. The RGO/PANI composite has almost the same peaks as pure PANI with slight shifts. In addition, it can be seen from Fig. 3(b) that the Raman peaks of the RGO/PANI nanocomposite at 1330 and 1589 cm^{-1}, which are respectively related to the D and G modes of RGO, are more pronounced than those of pure PANI.[17]

3.2 Humidity-sensing properties

The variations in the responses of the RGO/PANI humidity sensors with increasing RH are shown in Fig. 4(a). The response increases with increasing RH at the same applied voltage of

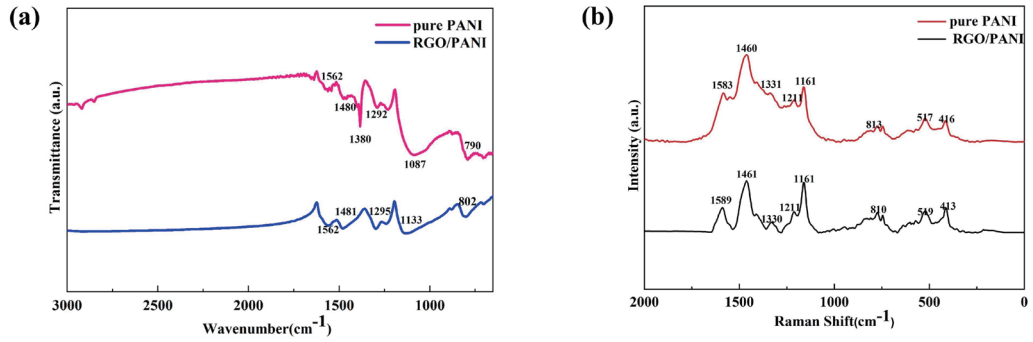

Fig. 3. (Color online) (a) FTIR spectra of PANI and RGO/PANI composite. (b) Raman spectra of PANI and RGO/PANI composite.

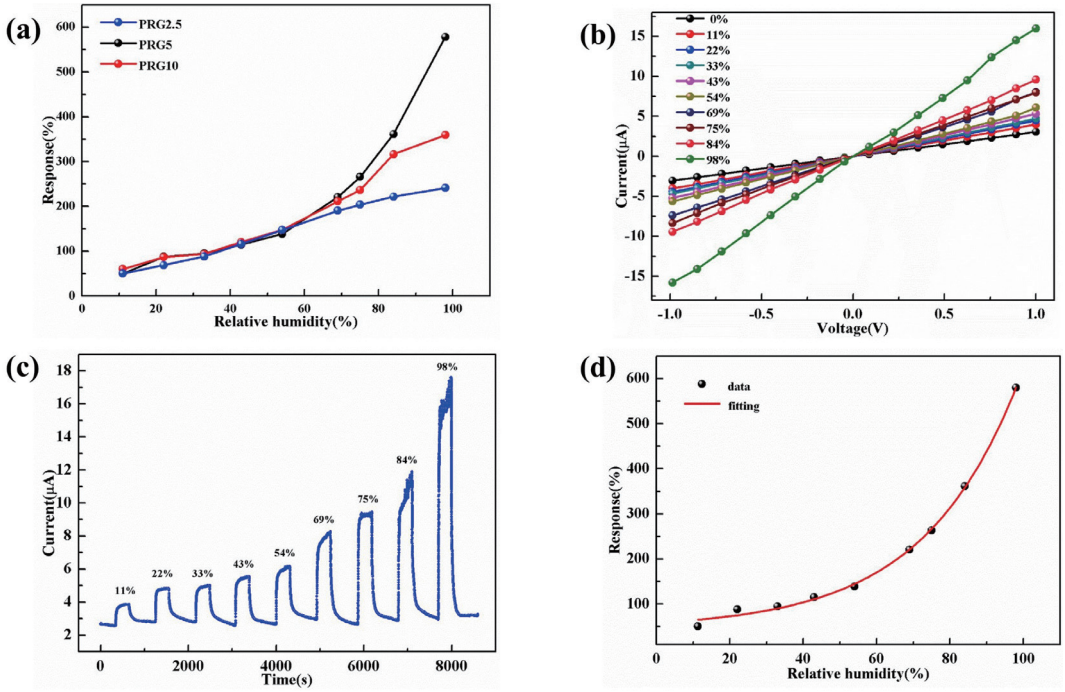

Fig. 4. (Color online) (a) Comparison of changes in responses of the PRG10, PRG5, and PRG2.5 humidity sensors in the RH range of 11–98%. (b) Electrical characterization of the PRG5 humidity sensor. (c) Sensing transient currents of the RGO/PANI humidity sensor at various RH levels. (d) Response of RGO/PANI humidity sensor as a function of RH in the range of 11–98%.

1 V. In addition, the content ratio of RGO to PANI has an important influence on the humidity response of the sensors. It can be seen that the curve of the PRG5 humidity sensor is the steepest, indicating the best response. Therefore, the PRG5 humidity sensor was selected in the subsequent measurements.

Figure 4(b) shows the current–voltage (*I*–*V*) relationships of the PRG5 humidity sensor after exposure to a wide range of RH levels (0–98% RH). The *I*–*V* curves clearly exhibit linear behavior, indicating that the electrode and the RGO/PANI composite film formed a good ohmic

contact. Therefore, the resistances of the humidity sensor at different RH levels can be obtained from the reciprocal of the slope of the *I*–*V* curves. As shown in Fig. 4(b), water adsorption decreases the resistance of the humidity sensor. For example, the resistance is reduced by about 89% when RH increases from 0% (388033 Ω) to 54% (41841 Ω).

Figure 4(c) shows the time-dependent response–recovery characteristic of the PRG5 humidity sensor to different RHs. During the test, the humidity sensor was switched between 0% RH and the tested RH. As can be seen, upon switching to a higher RH, the current of the sensor is greater. For example, the current increases from 2.58 to 17.53 μA when RH is increased from 0 to 98%. In addition, a higher RH leads to a greater response, with the greatest response of around 580% obtained at 98% RH. The response of the PRG5 humidity sensor shows an exponential dependence on RH, as shown in Fig. 4(d). The fitting equation of the response (y) versus RH (x) can be expressed as $y = 12e^{x/26} + 46$ and the coefficient of determination R^2 is 0.9972, indicating a very strong exponential trend.

To investigate the reversibility of the sensor, the transient current of the PRG5 humidity sensor was measured through humidity-increasing and humidity-decreasing cycles. In the humidity-increasing measurement, the sensor was switched between 0 and 11, 22, 33, 43, 54, 69, 75, 84, and 98% RH in turn, with the opposite sequence followed in the humidity-decreasing measurement, as shown in Fig. 5(a). In this process, the current of the sensor increased with increasing RH level and decreased with decreasing RH level, leading to the approximate symmetry of Fig. 5(a). The maximum humidity hysteresis is about 3% RH at 75% RH, indicating the good reversible property of the humidity sensor.

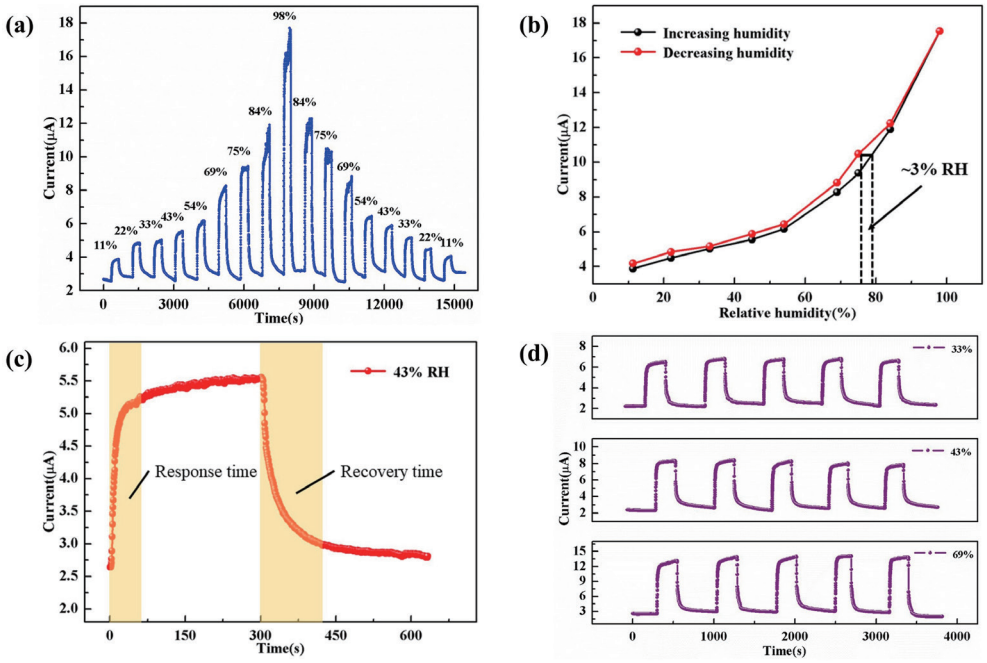

Fig. 5. (Color online) (a) Dynamic shift of current of the PRG5 humidity sensor when exposed to RH in the range of 0–98%. (b) Hysteresis of the PRG5 humidity sensor. (c) Response and recovery curves of the PRG5 humidity sensor at 43% RH. (d) Repeatability of the PRG humidity sensor exposed to 33, 43, and 69% RH.

Figure 5(c) shows the response and recovery behavior of the PRG5 humidity sensor toward 43% RH . The response time is about 70 s when RH is increased from 0 to 43%, whereas the corresponding recovery time is about 139 s when RH is decreased from 43 to 0%. These times are shorter than those of previously reported humidity sensors.[18–20]

Repeatability is also an important performance index for a sensor, with a lower repeatable error value indicating better repeatability. Figure 5(d) shows the repeatability of the PRG5 humidity sensor at 33, 43, and 69% RH over five cycles. There is no evident change in the current cycles of the sensor under the same testing condition, and the stable-state currents are about 6.7 μA (33% RH), 8.16 μA (43% RH), and 13.70 μA (69% RH), indicating that the humidity sensor has good repeatability.

Table 1 presents a comparison of the sensitivity of the proposed sensor with those of other previously reported humidity sensors. The response of the RGO/PANI composite film is greater than those of the other humidity sensors. By comparing the measurement range, hysteresis, and response, it is clear that the RGO/PANI nanocomposite film in our study shows good humidity-sensing performance.

3.3 Mechanism of humidity sensing

The Grotthuss mechanism can be used to explain the humidity sensing mechanism of the RGO/PANI composite sensor. When the humidity sensor is exposed to a low RH, only a few water molecules are physisorbed on the surface of the RGO/PANI composite via double hydrogen bonding, forming the first layer of physisorbed water molecules. At this stage, water molecules cannot move freely because of the constraint imposed by double hydrogen bonding, Therefore, the RGO/PANI composite exhibits a lower current at a lower RH. At a high RH, the adsorbed water molecules are in a multilayered, liquid-like configuration, and charge transport between neighboring water molecules by protons becomes feasible, which is known as the Grotthuss mechanism ($H_3O^+ + H_2O \rightarrow H_2O + H_3O^+$). Ionic transfer is the main conduction mode in this process, and the current increases with the RH. As a result, the rapid transfer of ions on the water layer sharply reduces the resistance.[25]

Table 1
Performance comparison of the proposed humidity sensor with other previously reported sensors.

Sensing material	Range	Hysteresis	Response	Reference
rGO/WS_2	0–91.5% RH	~3% RH	~17%	21
RGO/LS	22–97% RH	~5.6% RH	~298%	4
PANI/WO_3	10–85% RH	~6% RH	~200%	22
SiNWs	11.3–93% RH	~8.1% RH	~180%	23
KC/MWCNTs	10–90% RH	~4% RH	~90%	24
RGO/PANI	0–98% RH	~3% RH	~580%	Our work

4. Conclusions

We demonstrated a high-performance humidity sensor based on an RGO/PANI composite film. GO was reduced by $NaBH_4$, and then PANI was deposited in situ on RGO nanosheets by polymerizing aniline with APS to produce the RGO/PANI nanocomposite. The humidity-sensing properties of the sensor were investigated over a wide RH range (0–98%) at room temperature, and the sensor exhibited good adsorption and desorption characteristics when exposed to different RH levels, as well as excellent repeatability and reversibility. The good humidity-sensing behavior can be attributed to the synergistic effect between RGO and PANI.

Acknowledgments

This work was supported by Fundamental Research Funds for Central Universities (19CX02053A), the National Natural Science Foundation of China (No. 61890964), and the National Training Program of Innovation and Entrepreneurship for Undergraduates (20190472, 202012077).

References

1 M. T. S. Chani, K. S. Karimov, F. A. Khalid, S. Z. Abbas, and M. B. Bhatty: Chin. Phys. B **22** (2013) 010701. https://doi.org/10.1088/1674-1056/22/1/010701
2 M. H. Feng and X. J. Li: Sens. Actuators, B **272** (2018) 543. https://doi.org/10.1016/j.snb.2018.06.023
3 P. Sun, M. Wang, L. Liu, L. Jiao, W. Du, F. Xia, M. Liu, W. Kong, L. Dong, and M. Yun: Appl. Surf. Sci. **475** (2019) 342. https://doi.org/10.1016/j.apsusc.2018.12.283
4 C. Chen, X. Wang, M. Li, Y. Fan, and R. Sun: Sens. Actuators, B **255** (2018) 1569. https://doi.org/10.1016/j.snb.2017.08.168
5 X. Yu, X. Chen, X. Ding, X. Chen, X. Yu, and X. Zhao: Sens. Actuators, B **283** (2019) 761. https://doi.org/10.1016/j.snb.2018.12.057
6 C. Wang, L. Yin, L. Zhang, D. Xiang, and R. Gao: Sensors **10** (2010) 2088. https://doi.org/10.3390/s100302088
7 S. Wang, G. Xie, Y. Su, Q. Zhang, H. Du, H. L. Tai, and Y. D. Jiang: Sens. Actuators, B **255** (2018) 2203. https://doi.org/10.1016/j.snb.2017.09.028
8 Y. Li, K. Fan, H. Ban, and M. Yang: Synth. Met. **199** (2015) 51. https://doi.org/10.1016/j.synthmet.2014.11.009
9 X. Z. Li, S. R. Liu, and Y. Guo: RSC Adv. **6** (2016) 63099. https://doi.org/10.1039/C6RA10093G
10 M. Gnerlich, E. Pomerantseva, K. Gregorczyk, D. Ketchum, G. Rubloff, and R. Ghodssi: J. Micromech. Microeng. **23** (2013) 114014. https://doi.org/10.1088/0960-1317/23/11/114014
11 T. Kojić, G. M. Stojanović, A. Miletić, M. Radovanović, H. Al-Salami, and F. Arduini: Sens. Mater. **31** (2019) 2981. https://doi.org/10.18494/SAM.2019.2473
12 X. J. Lv, M. S. Yao, G. E. Wang, Y. Z. Li, and G. Xu: Sci. China Chem. **60** (2017) 1197. https://doi.org/10.1007/s11426-017-9079-5
13 A. M. Soomro, F. Jabbar, M. Ali, J. W. Lee, S. W. Mun, and K. H. Choi: J. Mater. Sci.-Mater. Electron. **30** (2019) 9455. https://doi.org/10.1007/s10854-019-01277-1
14 S. Bai, Y. Zhao, J. Sun, Y. Tian, R. Luo, D. Li, and A. Chen: Chem. Commun. **51** (2015) 7524. https://doi.org/10.1039/c5cc01241d
15 D. Zhang, D. Wang, X. Zong, G. Dong, and Y. Zhang: Sens. Actuators, B **262** (2018) 531. https://doi.org/10.1016/j.snb.2018.02.012
16 S. L. Patil, S. G. Pawar, M. A. Chougule, B. T. Raut, P. R. Godse, S. Sen, and V. B. Patil: Int. J. Polym. Mater. Polym. **61** (2012) 809. https://doi.org/10.1080/00914037.2011.610051
17 K. Wang, L. Li, Y. Liu, C. Zhang, and T. Liu: Adv. Mater. Interfaces **3** (2016) 1600665. https://doi.org/10.1002/admi.201600665
18 P. G. Su, W. L. Shiu, and M. S. Tsa: Sens. Actuators, B **216** (2015) 467. https://doi.org/10.1016/j.snb.2015.04.070

19 D. Zhang, J. Tong, and B. Xia: Sens. Actuators, B **197** (2014) 66. https://doi.org/10.1016/j.snb.2014.02.078
20 X. Zhang, D. Maddipatla, A. K. Bose, S. Hajian, B. B. Narakathu, J. D. Williams, M. F. Mitchell, and M. Z. Atashbar: IEEE Sens. J. **20** (2020) 12592. https://doi.org/10.1109/JSEN.2020.3002951
21 Z. H. Duan, Q. N. Zhao, C. Z. Li, S. Wang, Y. D. Jiang, Y. J. Zhang, B. H. Liu, and H. L. Tai: Rare Metals **40** (2021) 1762. https://doi.org/10.1007/s12598-020-01524-z
22 R. Kumar and B. C. Yadav: J. Inorg. Organomet. Polym. Mater. **26** (2016) 1421. https://doi.org/10.1007/s10904-016-0412-9
23 X. Chen, J. Zhang, Z. Wang, Q. Yan, and S. Hui: Sens. Actuators, B **156** (2011) 631. https://doi.org/10.1016/j.snb.2011.02.009
24 X. Peng, J. Chu, A. Aldalbahi, M. Rivera, L. Wang, S. Duan, and P. Feng: Appl. Surf. Sci. **387** (2016) 149. https://doi.org/10.1016/j.apsusc.2016.05.108
25 H. Bi, K. Yin, X. Xie, J. Ji, S. Wan, L. Sun, M. Terrones, and M. S. Dresselhaus: Sci. Rep. **3** (2013) 2714. https://doi.org/10.1038/srep02714